https://doi.org/10.1038/s41427-023-00486-9

NPG Asia Materials

ARTICLE Open Access

Zero-dimensionality of a scaled-down VO_2 metal-insulator transition via high-resolution electrostatic gating

Takeaki Yajima[1], Yusuke Samata[2], Satoshi Hamasuna[1], Satya Prakash Pati[1] and Akira Toriumi[2]

Abstract

An understanding of the phase transitions at the nanoscale is essential in state-of-the-art engineering[1–5], instead of simply averaging the heterogeneous domains formed during phase transitions[6,7]. However, as materials are scaled down, the steepness of the phase transition rapidly increases[8–13] and requires extremely high precision in the control method. Here, a three-terminal device, which could precisely control the phase transition electrically[14–19], was applied for the first time to a scaled-down metal-insulator transition material VO_2. The crossover from continuous to binary transitions with the scaled-down material was clarified, and the critical channel length was successfully elucidated via phase boundary energy. Notably, below the critical channel length, the spatial degrees of freedom degenerated, and the impact of drain voltage application disappeared in the phase transition, indicating zero-dimensionality of the VO_2 channel. This zero-dimensionality could be the fundamental property in the scaled-down phase transition and have a significant impact on various fields that need nanoscale engineering.

Introduction

Phase transition materials are important components of a wide range of functional devices, including memory, batteries, sensors, and neuromorphic computing[1–5]. During phase transitions, spatially heterogeneous domain structures are formed that affect material properties[6,7]. However, when phase transition materials are miniaturized to smaller than the size of individual domains, the phase transition becomes single-domain and exhibits different behavior[8–13]. Therefore, when designing functional devices using phase transition materials, it is essential to understand the effects of miniaturization.

Controlling phase transitions using a three-terminal device[14–16] can provide a novel opportunity for the study of scaled-down phase transitions, as shown in Fig. 1a. The three-terminal device can control the phase transition by applying a gate voltage to an insulating layer to accumulate electrons or holes in the phase transition material. It can electrically modulate the carrier concentration in the phase transition material, changing the free energy balance between phases and inducing the phase transition. Unlike simple two-terminal devices, the control terminals are completely isolated by an insulating layer, enabling control in a quasi-equilibrium state in a similar way to thermodynamic phase control. Controlling phases using three-terminal devices is a long-standing challenge in materials science and has been studied from various approaches, as represented by research on Mott transistors[17–19]. Some approaches using liquid gates can accumulate a large amount of charge using the electric double layer at the solid−liquid interface and achieve a large control range[18,19]. However, they also have the fatal problem of unexpected electrochemical reactions, causing a complicated interpretation of the results[20]. On the other hand, those using solid gate dielectrics can achieve highly precise control near the transition point, although the control range is relatively small[15,16]. For example, a

Correspondence: Takeaki Yajima (yajima@ed.kyushu-u.ac.jp)
[1]Department of Electrical and Electronic Engineering, Kyusyu University, Motooka 744, Fukuoka 819-0395, Japan
[2]Department of Materials Engineering, The University of Tokyo, Bunkyo 7-3-1, Tokyo 113-8654, Japan

© The Author(s) 2023

Open Access This article is licensed under a Creative Commons Attribution 4.0 International License, which permits use, sharing, adaptation, distribution and reproduction in any medium or format, as long as you give appropriate credit to the original author(s) and the source, provide a link to the Creative Commons license, and indicate if changes were made. The images or other third party material in this article are included in the article's Creative Commons license, unless indicated otherwise in a credit line to the material. If material is not included in the article's Creative Commons license and your intended use is not permitted by statutory regulation or exceeds the permitted use, you will need to obtain permission directly from the copyright holder. To view a copy of this license, visit http://creativecommons.org/licenses/by/4.0/.

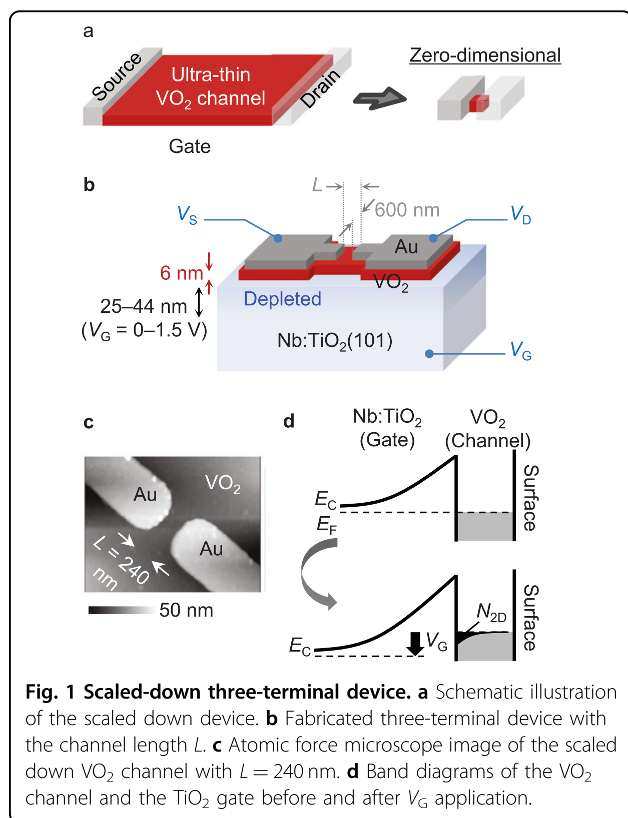

Fig. 1 Scaled-down three-terminal device. a Schematic illustration of the scaled down device. **b** Fabricated three-terminal device with the channel length L. **c** Atomic force microscope image of the scaled down VO_2 channel with $L = 240$ nm. **d** Band diagrams of the VO_2 channel and the TiO_2 gate before and after V_G application.

voltage control of 10 mV step corresponds to ultrahigh-precision control of several mK steps when converted to temperature. However, despite such promising properties, research using solid-state three-terminal devices is still in its infancy, and there has been no example of its application to the scaled-down phase transition. Past literature on VO_2 three-terminal devices has used relatively long channels above 1 μm (see Fig. S1 in Supplementary Information for details) and has never systematically considered the scaling effect with the exception of only the channel width dependence[21].

In this study, we focused on the metal-insulator transition of VO_2 and systematically evaluated the effect of miniaturization using a three-terminal device. VO_2 is a material that has been used in various applications, such as infrared sensors[4], thermistors[22], switches[23], and neuromorphic elements[24], because it induces a phase transition in a convenient temperature range above room temperature and changes electrical resistance by three orders of magnitude[25]. In a study of VO_2 using a three-terminal device, the phase transition of the VO_2 channel could be continuously controlled from the insulating state to the metallic state by applying a gate voltage near the transition temperature via TiO_2 gate dielectrics[15,16]. Here, we found that scaling down the VO_2 channel to the sub-μm scale resulted in a completely binary switching behavior instead of a continuous transition. The scaling-down effect was also successfully simulated by the phase transition transistor model, and the critical channel length could be explained by the phase boundary energy. Below the critical channel length, the spatial degrees of freedom of the channel degenerated, and the effect of drain voltage on the phase transition was nullified, showing zero-dimensionality as one of the most fundamental properties of scaled-down phase transitions.

Materials and methods

A schematic diagram of the fabricated device is shown in Fig. 1b. A 6 nm VO_2 thin film was epitaxially grown on the Nb-doped TiO_2 substrate and patterned as a channel. The source and drain electrodes were fabricated with the channel length ($L = 240$ or 490 nm) and the channel width ($W = 600$ nm), as shown in the atomic force microscope image in Fig. 1c. As shown in the band diagram in Fig. 1d, the Nb-doped TiO_2 substrate was the gate electrode, and its interface region with the VO_2 channel was depleted by several tens of nanometers, which could be viewed as a gate dielectric layer that isolates the gate from the channel. When a positive voltage was applied on the gate, the depletion layer expanded, and electrons accumulated in the VO_2 channel, which could induce a metallic transition. The accumulated electron density with respect to $V_G = 0$ V could be estimated as 1.9×10^{13} cm^{-2} at a V_G of 1 V and 4.4×10^{13} cm^{-2} at a V_G of 3 V (ref. [16]). The relative dielectric constant of TiO_2 (perpendicular to the (101) plane) was approximately 111, which was much higher than that of SiO_2 or high-k materials[15]. The depletion layer rather than the entire substrate was used as the gate insulator. These two factors enabled the accumulation of a large number of electrons in our solid-state device, which was a unique characteristic of our device.

Methods

Device fabrication

A 6 nm VO_2 thin film was epitaxially grown on a Nb 0.05 wt% doped TiO_2 (101) substrate via pulsed laser deposition. The Au electrodes for the source and the drain were formed via e-beam lithography and lift-off. Then, a resist mask of the VO_2 pattern was created, and the VO_2 was etched with 0.4 M $NaIO_4$ solution. As shown in the atomic force microscope image in Fig. 1c, the width of the Au electrode near the VO_2 channel W is 600 nm, and the distance between the Au electrodes L is 240 nm or 490 nm for two different devices.

Results

Transfer characteristics

Figure 2 shows the temperature dependence and transfer characteristics of several devices with different channel lengths L. Figures 2a and 2d show the results for

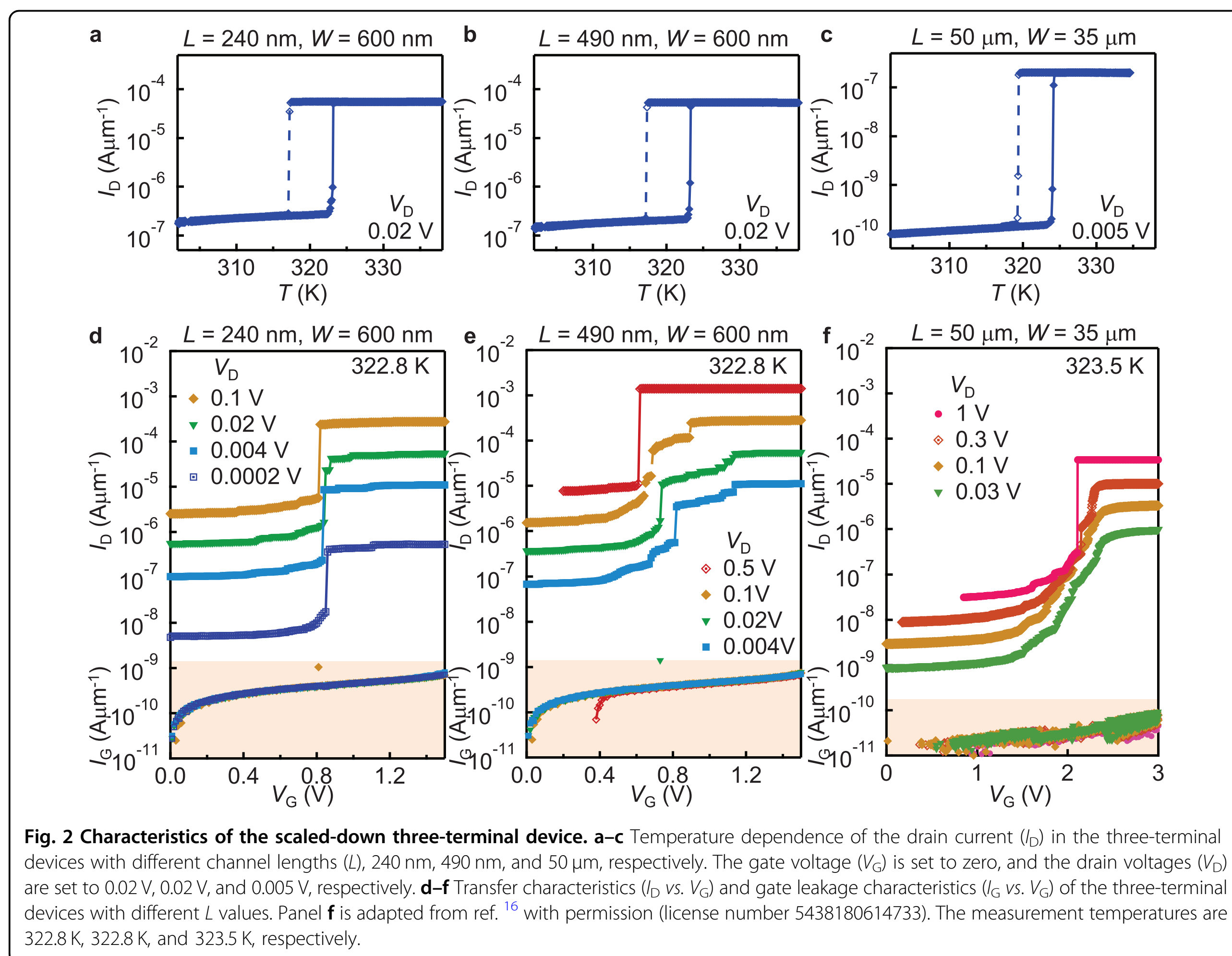

Fig. 2 Characteristics of the scaled-down three-terminal device. a–c Temperature dependence of the drain current (I_D) in the three-terminal devices with different channel lengths (L), 240 nm, 490 nm, and 50 µm, respectively. The gate voltage (V_G) is set to zero, and the drain voltages (V_D) are set to 0.02 V, 0.02 V, and 0.005 V, respectively. **d–f** Transfer characteristics (I_D *vs.* V_G) and gate leakage characteristics (I_G *vs.* V_G) of the three-terminal devices with different L values. Panel **f** is adapted from ref. [16] with permission (license number 5438180614733). The measurement temperatures are 322.8 K, 322.8 K, and 323.5 K, respectively.

an L of 240 nm, and Figs. 2b and 2e show the results for an L of 490 nm. For comparison, the characteristics for the L of 50 µm device in ref. [16] are also shown in Figs. 2c and 2f with permission. As shown in Fig. 2a-c, the temperature dependence of the VO_2 channel showed that there was a steep resistance change at approximately 320 K, irrespective of the L values. However, the temperature step of the measurement could not be lower than 50 mK due to temperature fluctuations, and the detailed L dependence could not be evaluated. Therefore, we set the temperature near the transition point and measured the gate voltage dependence, which achieved much higher accuracy. Figure 2f shows the drain current (I_D) vs. the gate voltage (V_G) for an L of 50 µm ($W = 35$ µm). The 10 mV step in V_G corresponded to a 3 mK step in temperature[15,16] and showed that the transition was essentially continuous (see the plot for 0.03 V drain voltage (V_D)), although it was steep in the temperature dependence. This continuous transition meant that the channel size was sufficiently larger than the domain size of the phase transition, and the averaged characteristics of many domains with different transition temperatures were observed. Moreover, Fig. 2d shows I_D vs. V_G for the L of 240 nm device. The drain current jumped discontinuously even with high-precision measurement via V_G (see the plot of $V_D = 0.0002$ V). This results indicated that the domain size of the phase transition was comparable to the channel length, and the entire VO_2 channel collectively metallized. In the L of 490 nm device ($V_D = 0.004$ V), a partial discontinuity was observed, with a continuous resistance change at the same time. This result occurred because the channel size was slightly larger than the domain size of the phase transition and two types of extreme characteristics were mixed. Thus, the gate voltage dependence successfully elucidated the miniaturization effect in detail.

Although the use of a three-terminal device enabled highly precise control of the phase transition, the effect of V_D, which was unique to three-terminal devices, needed to be considered correctly. From Fig. 2f, the transfer characteristics significantly changed as V_D increased, and the continuous transition became discontinuous above a V_D of 0.3 V. The origin of this discontinuity was

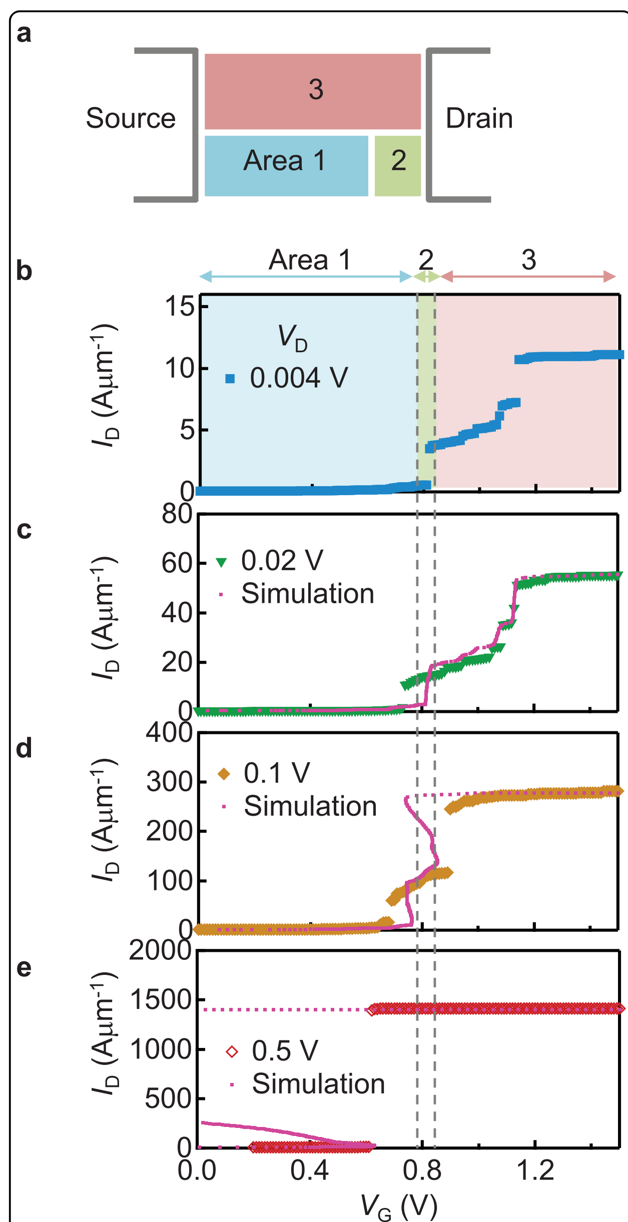

Fig. 3 Simulation for the intermediate channel length.
a Simulation conditions with three different areas in the $L = 490$ nm VO_2 channel. The following assumptions are made: Area 1 has a relatively low transition temperature and shows a continuous transition, Area 2 undergoes a discontinuous collective transition after the metallization of Area 1, and Area 3 exhibits multiple discontinuous transitions after the metallization of Area 2. Our proposed domain structure is just one of the various possible domain structures reproducing the experimental data. **b** Experimental data of the transfer characteristics at $V_D = 0.004$ V. The transfer curve is divided into three V_G regions (blue, green, and red shadows), and the I_D variation in each region is attributed to the metallic transition in Areas 1, 2, and 3, respectively. **c, d, e** Experimental data (mark) and simulated data (pink dot) of the transfer characteristics at $V_D = 0.02$ V, 0.1 V, and 0.5 V, respectively.

investigated in detail in a previous paper[13], which found that the gate-induced metallic transition triggered the positive feedback of Joule heating under the application of a large V_D and resulted in a discontinuous transition. However, in the scaled-down VO_2 channel (Fig. 2d), the effect of V_D was almost negligible because in miniaturized devices, the metallic transition collectively proceeded throughout the VO_2 channel, without the capacity for the positive feedback of Joule heating. In fact, the threshold V_G for the metallic transition in Fig. 2d hardly changed with increasing V_D. Thus, the metallic transition, which was initiated by the gate voltage, spread across the entire channel due to the collective nature of the phase transition. In other words, the spatial degree of freedom of the channel was degenerated, and the effect of the drain voltage was nullified, leading to a simple binary ON-OFF operation.

Simulation for intermediate channel length

In the case of the L of 490 nm device in Fig. 2e, the characteristics of continuous and discontinuous transitions were mixed, and the effect of V_D was more complicated. To verify whether the characteristics for $L = 490$ nm were consistent with the phase transition transistor model[16], we performed simulations, as shown in Fig. 3. Although the accurate domain structure was unknown, we divided the VO_2 channel into three areas, and Fig. 3a shows an example to approximately reproduce the main features in Fig. 2e. Based on the characteristics for the sufficiently small V_D (0.004 V) in Fig. 3b, three following assumptions were made: Area 1 had a relatively low transition temperature and showed a continuous transition, Area 2 underwent a discontinuous collective transition after the metallization of Area 1, and Area 3 exhibited multiple discontinuous transitions after the metallization of Area 2. With these assumptions, we could approximately reproduce the main features of the experimental data, as shown in Figs. 3c, 3d, and 3e (pink dots). See Fig. S2 in the Supplementary Information for more details. In the simulated plot, the negative transconductance region was observed where I_D increased as V_G decreased. This region was actually unstable against fluctuations and led to a discontinuous jump, as observed in the experimental data[16]. Thus, the seemingly complex transfer characteristics at $L = 490$ nm could be understood as an intermediate between two extreme limits.

Discussion

The phase diagrams of the VO_2 channel for different L values are summarized in Figs. 4a and 4b. In the long channel (Fig. 4b), a continuous transition governed by spatial heterogeneity was observed, while a discontinuous transition occurred with an increased V_D. However, in the scaled-down channel (Fig. 4a), the discontinuous

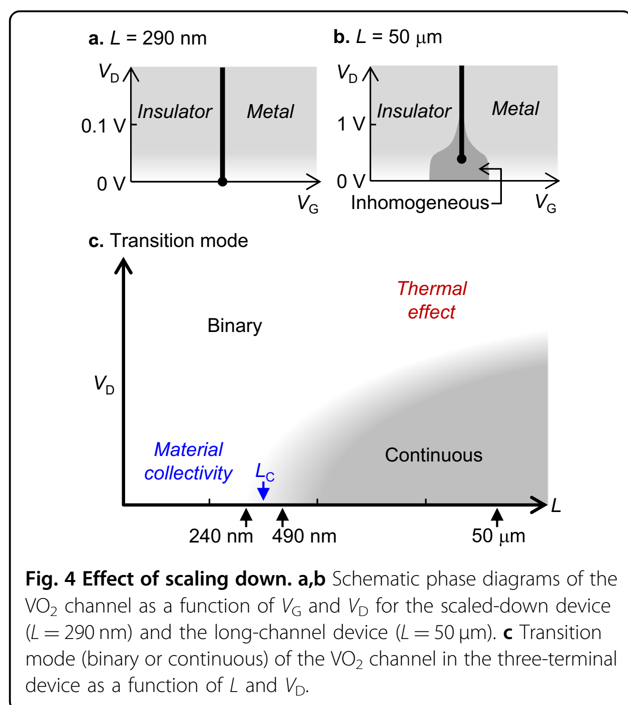

Fig. 4 Effect of scaling down. a,b Schematic phase diagrams of the VO_2 channel as a function of V_G and V_D for the scaled-down device ($L = 290$ nm) and the long-channel device ($L = 50$ μm). **c** Transition mode (binary or continuous) of the VO_2 channel in the three-terminal device as a function of L and V_D.

transition was originally achieved, and no change was observed with the increase in V_D. Specifically, the behavior of the scaled-down three-terminal device was simplified to a binary ON/OFF switching operation regardless of the magnitude of V_D.

The behavior of the gate-induced phase transition is shown for channel lengths L and the drain voltage V_D in Fig. 4c. The heterogeneous continuous transition and the collective binary transition were separated by the critical channel length L_C, which could be regarded as the static domain size of the phase transition. According to the past literature[7], the static domain size depended on two competing factors: heterogeneity (spatial fluctuations of free energy) and domain boundary energy. The heterogeneity could be inferred from the transition width of the long channel device as $\Delta T_{MIT} \sim 0.15$ K in terms of temperature. Then, the heterogeneity in terms of free energy could be calculated as $S_{MIT}\Delta T_{MIT}$, where S_{MIT} is the entropy difference between the metallic phase and the insulating phase; this was reported to be 9×10^5 JK^{-1}m^{-2} (ref. [26]). For the domain boundary energy E_b, a value of 0.03 Jm^{-2} was used as a reference[27,28]. Then, the critical channel length (or domain size) was approximately given by the ratio of these two factors as $L_C = E_b/(S_{MIT}T_{MIT})$ (ref. [28]). This equation could be interpreted in the following way: a larger E_b correlated to a larger domain size (L_C) due to the suppression of domain boundary formation and a larger heterogeneity (T_{MIT}) correlated to a smaller L_C due to the potential for an individual transition at each location. This equation led to an L_C of 340 nm and was consistent with the experimental results. Specifically, the scaled-down VO_2 channel underwent a collective transition due to the instability of the phase boundary.

Conclusion

In summary, we evaluated the metal-insulator transition of a scaled-down VO_2 channel using a three-terminal device that enabled electrical control with high precision. The results showed a crossover from a continuous transition to a simple binary transition with the scaled-down material. This observation was only possible due to the extreme high precision of the three-terminal control; in the temperature control, the transition of the VO_2 channel appeared to be steep regardless of the channel length due to its coarse precision. The spatial degree of freedom in the channel was found to degenerate with miniaturization, and the impact of drain voltage application disappeared in the phase transition. This meant that the channel effectively became zero-dimensional, which was a unique property of the scaled-down phase transitions. Zero-dimensionality of phase transitions, which nullified some of the applied stimuli, could facilitate the development of state-of-the-art devices and materials, delivering a significant impact on a wide range of science and engineering.

Acknowledgements
This research was supported by JSPS KAKENHI 20H02615 and was also partially supported by the Japan Science and Technology Agency (Grant No. JPMJCR19K2).

Author contributions
T.Y. and Y.S. performed device fabrication, measurements, and analyses. T.Y. performed the simulation, and S.H., S.P.P., and A.T. contributed to planning and discussion.

Data availability
The data that support the findings of this study are available from the authors upon reasonable request.

Conflict of interest
The authors declare no competing interests.

Publisher's note
Springer Nature remains neutral with regard to jurisdictional claims in published maps and institutional affiliations.

Supplementary information The online version contains supplementary material available at https://doi.org/10.1038/s41427-023-00486-9.

Received: 24 January 2023 Revised: 18 April 2023 Accepted: 20 April 2023.
Published online: 30 June 2023

References

1. Yuasa, S., Nagahama, T., Fukushima, A., Suzuki, Y. & Ando, K. Giant room-temperature magnetoresistance in single-crystal Fe/MgO/Fe magnetic tunnel junctions. *Nat. Mater.* **3**, 868–871 (2004).
2. Scott, J. F. & Araujo, C. A. P. Ferroelectric memories. *Science* **246**, 1400–1405 (1989).

3. Kim, S.-W., Seo, D.-H., Ma, X., Ceder, G. & Kang, K. Electrode materials for rechargeable sodium-ion batteries: potential alternatives to current lithium-ion batteries. *Adv. Energy Mater.* **2**, 710–721 (2012).
4. Jerominek, H. et al. Micromachined uncooled VO_2-based IR bolometer arrays. *Proc. Infrared Detect. Focal Plane Arrays Iv.* **2746**, 60–71 (1996).
5. Tuma, T., Pantazi, A., Gallo, M. L., Sebastian, A. & Eleftheriou, E. Stochastic phase-change neurons. *Nat. Nanotech.* **11**, 693–699 (2016).
6. Song, Y., Chen, X., Dabade, V., Shield, T. W. & James, R. D. Enhanced reversibility and unusual microstructure of a phase-transforming material. *Nature* **502**, 85–88 (2013).
7. Yajima, T., Ninomiya, Y., Nishimura, T. & Toriumi, A. Drastic change in electronic domain structures via strong elastic coupling in VO2 films. *Phys. Rev. B.* **91**, 205102 (2015).
8. Cowburn, R. P., Koltsov, D. K., Adeyeye, A. O., Welland, M. E. & Tricker, D. M. Single-domain circular nanomagnets. *Phys. Rev. Lett.* **83**, 1042–1045 (1999).
9. Lopez, R., Haynes, T. E., Boatner, L. A., Feldman, L. C. & Haglund, R. F. Jr Size effects in the structural phase transition of VO2 nanoparticles. *Phys. Rev. B.* **65**, 224113 (2002).
10. Zhai, H.-Y. et al. Giant discrete steps in metal-insulator transition in perovskite manganite wires phys. *Phys. Rev. Lett.* **97**, 167201 (2006).
11. Krause, S. et al. Magnetization reversal of nanoscale islands: how size and shape affect the arrhenius prefactor. *Phys. Rev. Lett.* **103**, 020404 (2014).
12. Sinwani, O., Reiner, J. W. & Klein, L. Monitoring superparamagnetic Langevin behavior of individual SrRuO3 nanostructures. *Phys. Rev. B.* **89**, 100403 (2012).
13. Tsuji, Y., Kanki, T., Murakami, Y. & Tanaka, H. Single-step metal–insulator transition in thin film-based vanadium dioxide nanowires with a 20 nm electrode gap. *Appl. Phys. Exp.* **12**, 025003 (2019).
14. Ahn, C. H., Triscone, J.-M. & Mannhart, J. Electric field effect in correlated oxide systems. *Nature* **424**, 1015–1018 (2003).
15. Yajima, T., Nishimura, T. & Toriumi, A. Positive-bias gate-controlled metal–insulator transition in ultrathin VO2 channels with TiO2 gate dielectrics. *Nat. Commun.* **6**, 10104 (2015).
16. Yajima, T. & Toriumi, A. Observation of the Pinch-Off Effect during Electrostatically Gating the Metal-Insulator Transition. *Adv. Elec. Mater.* **8**, 2100842 (2021).
17. Eblen-Zayas, M., Bhattacharya, A., Staley, N. E., Kobrinskii, A. L. & Goldman, A. M. Ambipolar gate effect and low temperature magnetoresistance of ultrathin La0.8Ca0.2MnO3 films. *Phys. Rev. Lett.* **94**, 037204 (2005).
18. Bollinger, A. T. et al. Superconductor–insulator transition in La2 2 xSrxCuO4 at the pair quantum resistance. *Nature* **472**, 458–460 (2011).
19. Nakano, M. et al. Collective bulk carrier delocalization driven by electrostatic surface charge accumulation. *Nature* **487**, 459–462 (2012).
20. Jeong, J. et al. Suppression of metal-insulator transition in VO2 by electric field–induced oxygen vacancy formation. *Science* **339**, 1402–1405 (2013).
21. Sasaki, T., Ueda, H., Kanki, T. & Tanaka, H. Electrochemical gating-induced reversible and drastic resistance switching in VO_2 nanowires. *Sci. Rep.* **5**, 17080 (2015).
22. Yajima, T., Tanaka, T., Samata, Y., Uchida, K. & Toriumi, A. High-speed low-energy heat signal processing via digital-compatible binary switch with metal-insulator transitions. *IEEE Int. Electron Devices Meet.* **19**, 903–906 (2019).
23. Zhou, Y. & Ramanathan, S. Mott memory and neuromorphic devices. *Proc. Ieee.* **103**, 1289–1310 (2015).
24. Yi, W. et al. Biological plausibility and stochasticity in scalable VO2 active memristor neurons. *Nat. Commun.* **9**, 4661 (2018).
25. Morin, F. J. Oxide which show a metal-to-insulator transition at the Neel temperature. *Phys. Rev. Lett.* **3**, 34–36 (1959).
26. Park, J. H. et al. Measurement of a solid-state triple point at the metal–insulator transition in VO2. *Nature* **500**, 431–434 (2013).
27. Wu, J. et al. Strain-induced self organization of metal-insulator domains in single-crystalline VO 2 nanobeams. *Nano Lett.* **6**, 2313–2317 (2006).
28. Yajima, T., Nishimura, T. & Toriumi, A. Identifying the collective length in VO2 metal–insulator transitions. *Small* **13**, 1603113 (2017).